Tetrahedron Letters 55 (2014) 1342–1346

Contents lists available at ScienceDirect

Tetrahedron Letters

journal homepage: www.elsevier.com/locate/tetlet

Anthracene-labeled pyridinium-based symmetrical chiral chemosensor for enantioselective recognition of L-tartrate

Kumaresh Ghosh *, Tanmay Sarkar

Department of Chemistry, University of Kalyani, Kalyani, Nadia 741235, India

ARTICLE INFO

Article history:
Received 21 October 2013
Revised 3 January 2014
Accepted 7 January 2014
Available online 10 January 2014

Keywords:
Anthracene-labeled symmetric chiral sensor
Enantioselective recognition
Sensing of L-tartrate
Fluorometric discrimination
Pyridinium amide
L-Valine as chiral source

ABSTRACT

A new anthracene-based chiral chemosensor **1** has been designed and synthesized. L-Valine has been used as the chiral source in the design. The chemosensor **1** has been established as an efficient enantioselective sensor for L-tartrate. While in the presence of L-tartrate the fluorescent sensor **1** in DMSO exhibits considerable increase in emission, the isomeric tartrate brings relatively small change. The enantiomeric fluorescence difference ratio (*ef*) has been determined to be 29.38.

Synthetic fluorescent chemosensor that discriminates the enantiomers of a particular chiral guest by exhibiting different fluorescence behaviors draws attention in the area of molecular recognition.[1] Now-a-days fluorescence technique is widely used over the other different analytical methods, as fluorescence-based enantioselective sensors can provide high sensitivity and real-time measurement.[2] In the past several years, there has been an interest in the enantioselective recognition of α-hydroxycarboxylic acids[1a,3] due to their presence as the structural unit of many natural products and drug molecules. They can also serve as the multifunctional precursors to a great variety of organic compounds.[4] Among the different hydroxyl carboxylic acids, tartaric acid is a common natural product present in wines and other grape-derived beverages. Large accumulation of tartaric acid causes human fatality with death. Therefore, recognition of this molecule especially its anionic form is important. Scrutiny of the literature reveals that hydrogen bonding receptors for both neutral[5] and anionic[6] forms of tartaric acid or its derivatives are known. Very few reports are available for chiral recognition of the anionic form of tartaric acid in the literature. Recently, we have reported L-valine derived benzimidazole based urea molecule that fluorometrically discriminates L-tartrate from its D-isomer in DMSO.[7] The inspiring results have prompted us further to undertake a new design which is comprised of pyridinium amide motifs. In this regard, we herein report the design, synthesis and chiral recognition properties of L-valine coupled anthracene labeled pyridinium-based symmetrical sensor **1**. The chiral chemosensor **1** shows good fluorometric discrimination between L- and D-tartrates in DMSO.

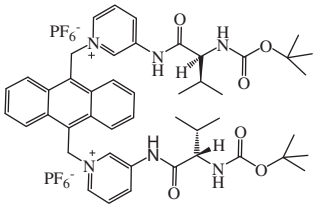

1

Scheme 1 describes the synthesis of sensor **1**. Initially, *N*-Boc-L-valine acid **2** derived from *N*-Boc-L-valine ester, was coupled with 3-aminopyridine to afford the compound **3**. Then quaternization of the pyridine ring nitrogen in **3** using 9,10-bis(chloromethyl)anthracene followed by exchange of Cl^- ions with PF_6^- ions introduced the chemosensor **1**. All the compounds were characterized by ^1H NMR, ^{13}C, FTIR, and mass analyses.

The solution phase binding interaction of **1** with the tetrabutylammonium salts of D-/L-tartaric and *R*-/*S*-mandelic acids was investigated in DMSO by UV–vis and fluorescence techniques. The chemosensor **1** in DMSO showed an intense emission at 432 nm when excited at 380 nm. However, upon progressive addition of the tetrabutylammonium salts of D-/L-tartaric and *R*-/*S*-mandelic acids to the solution of **1** ($c = 1.12 \times 10^{-4}$ M) in DMSO,

* Corresponding author. Fax: +91 33 2582 8282.
E-mail address: ghosh_k2003@yahoo.co.in (K. Ghosh).

0040-4039/$ - see front matter © 2014 Elsevier Ltd. All rights reserved.
http://dx.doi.org/10.1016/j.tetlet.2014.01.016

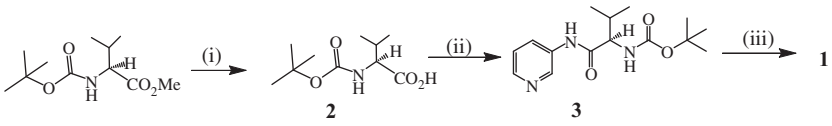

Scheme 1. Reagents and conditions: (i) LiOH, MeOH–H_2O, stirring, 4 h; (ii) 3-aminopyridine, DCC, DMAP, dry CH_2Cl_2, stirring, 19 h; (iii) (a) 9,10-bis(chloromethyl)anthracene, CH_3CN, reflux, 72 h; (b) NH_4PF_6, MeOH/H_2O.

the intensity of monomer emission at 432 nm suffered change to different extents. During fluorometric titration with L-tartrate, the emission of **1** at 432 nm increased significantly and it was distinguishable from its D-isomer. In relation to this, the fluorescence ratio of **1** at 432 nm for all anions except L-tartrate was found to be negligible in magnitude.

Figure 1 shows the change in fluorescence ratio of **1** in the presence of 20 equiv amounts of tetrabutylammonium salts of D-/L-tartaric and *R*-/*S*-mandelic acids in DMSO. As can be seen from Figure 1, although the enantiomers of mandelate are hardly discriminated, receptor **1** shows sharp fluorometric discrimination between D- and L-tartrates.

Figure 2a and b show the change in emission of **1** upon increasing the addition of tetrabutylammonium salts of D-/L-tartaric acids in DMSO, respectively. From Figure 2a, it is clear that upon gradual addition of L-tartrate ($c = 2.2 \times 10^{-3}$ M) to the receptor solution in DMSO, the emission intensity at 432 nm is considerably enhanced. In contrast, upon addition of D-tartrate ($c = 2.2 \times 10^{-3}$ M) the emission intensity in the same region is initially decreased and then increased (Fig. 2b). Such initial decrease in emission followed by a recovery reflects the different binding modes due to which, the photoinduced electron transfer (PET) occurring in-between the binding site and the excited state of anthracene is regulated in different ways. We believe that the initial decrease in emission is due to the hydrogen bonding interaction of the individual arm of **1**. During the titration, in the presence of excess concentration of D-tartrate, a conformational change takes place due to which the bridging of the two binding arms occurs and the emission is regulated in the increasing mode. This is supported by the observation noted in emission titration using *R*-/*S*-mandelates. Under similar conditions, enantiomers of mandelate quenched the emission to smaller extents (Supporting information).

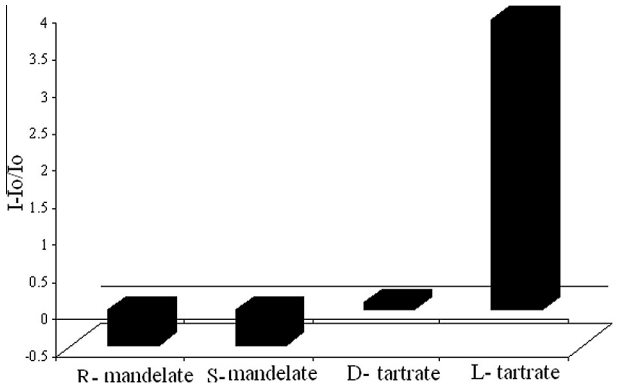

Figure 1. Change in fluorescence ratio of **1** ($c = 1.12 \times 10^{-4}$ M) at 432 nm upon addition of 20 equiv amounts of anions.

Time-resolved fluorescence decay profile of **1** in DMSO with L- and D-tartrates shows different behaviors. The decay curve for **1** monitored at 440 nm ($\lambda_{exc} = 380$ nm) was fitted to a three exponential decay with a major (1.24 ns, 68.66%) and minor components (76.4 ps, 18.50%; 4.87 ps, 12.84%). While in the presence of L-tartrate the decay curve of **1** fits to three exponential decay, under similar conditions in the presence of D-tartrate it fits to two exponential decay (Supporting information). In the decay profile of **1**, the major component for anthracene (lifetime 1.24 ns) shows significant increase in lifetime in the presence of D- and L-tartrates and contributes to the total fluorescence with different pre-exponential factors. This indicated the different interaction behaviors of **1** toward L- and D-tartrates in the excited state.

However, in the emission titration spectra of **1** with all the guests small inflection at ~525 nm was noticed. This is presumably attributed to the guest chelation induced formation of intermolecular anthracene excimer[8] which disappears upon strong interaction with L-tartrate.

The selective recognition effect on the guest of the D-/L-isomers of tartrate was understood from the enantiomeric fluorescence difference ratio, $ef[ef = (I_L - I_0)/(I_D - I_0)]$. I_0 represents the fluorescence emission intensity in the absence of the chiral substrate. I_L

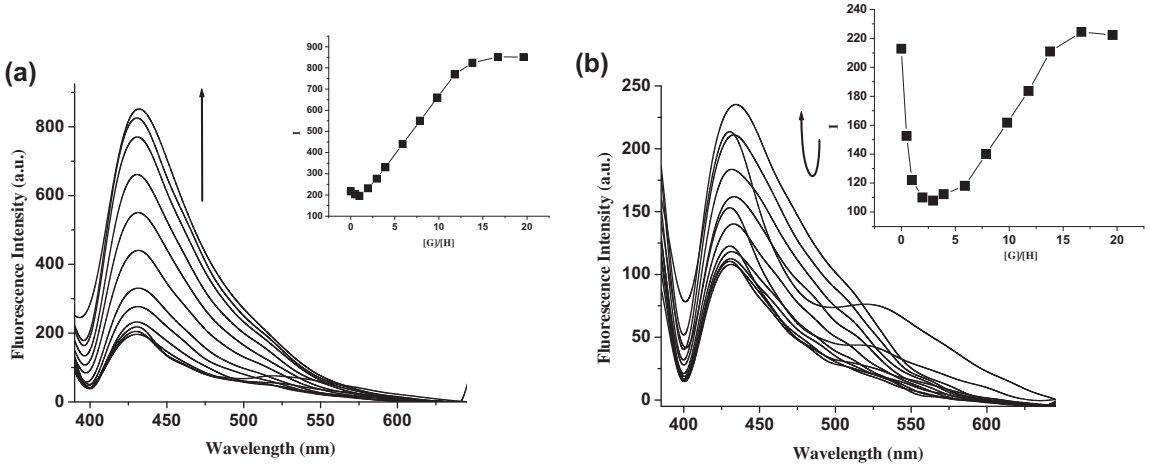

Figure 2. Fluorescence titration spectra of **1** ($c = 1.12 \times 10^{-4}$ M) in DMSO upon addition of tetrabutylammonium salts of (a) L-tartaric (Inset: change in emission at 432 nm with $[G]/[H]$) and (b) D-tartaric acids (concentration of guests was 2.2×10^{-3} M) ($\lambda_{exc} = 380$ nm).

and I_D are the fluorescence intensities in the presence of L- and D-tartrates, respectively. The value of '*ef*' is determined to be 29.38 for the chemosensor **1**. This large value of '*ef*' signifies that chemosensor **1** exhibits a good enantioselective response toward L-tartrate. The steric fit of the L-isomer into the *syn* conformation of **1** presumably indicates strong hydrogen bonding interaction. The equilibrium *anti* conformation **1X**[9] will go to the *syn* conformation **1Y** in the presence of tartrate (dicarboxylates) due to the formation of greater number of hydrogen bonds (Fig. 3).

To be confirmed with the suggested mode of interaction in Figure 3, ^{1}H NMR studies of **1** in the presence of equiv amounts of L- and D-tartrates were done in d_6-DMSO (Fig. 4). The amide proton H_a and carbamate proton H_f in **1** underwent downfield chemical shift during complexation. The pyridinium ring protons H_b and H_c moved much to the downfield directions and thereby indicated their involvement in complexation. Careful study reveals that the chemical shift of the indicated protons is slightly more in the presence of L-tartrate than observed with D-tartrate.

DFT calculations of the complexes of **1** with both D- and L-tartrates in the gas phase were further carried out to realize the hydrogen bonding interaction in the ground state.[10] It has been noticed that the complex of L-tartrate is slightly stable than its isomeric complex by −0.30 kcal/mol. This small energy difference between the complexes corroborates the small efficiency of **1** in discrimination between L- and D-tartrates in the ground state. Figure 5 reveals the DFT optimized geometries with corresponding hydrogen bonding features.

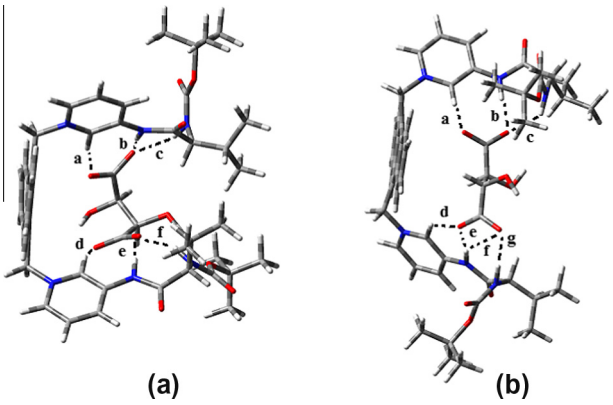

Figure 5. DFT optimized geometries of the complexes of **1** with (a) L-tartrate (hydrogen bond distances: a = 1.80 Å, b = 1.58 Å, c = 2.06 Å, d = 1.95 Å, e = 1.58 Å, f = 1.73 Å and (b) D-tartrate (hydrogen bond distances: a = 1.74 Å, b = 1.71 Å, c = 2.07 Å, d = 2.03 Å, e = 1.60 Å, f = 2.95 Å, g = 1.84 Å).

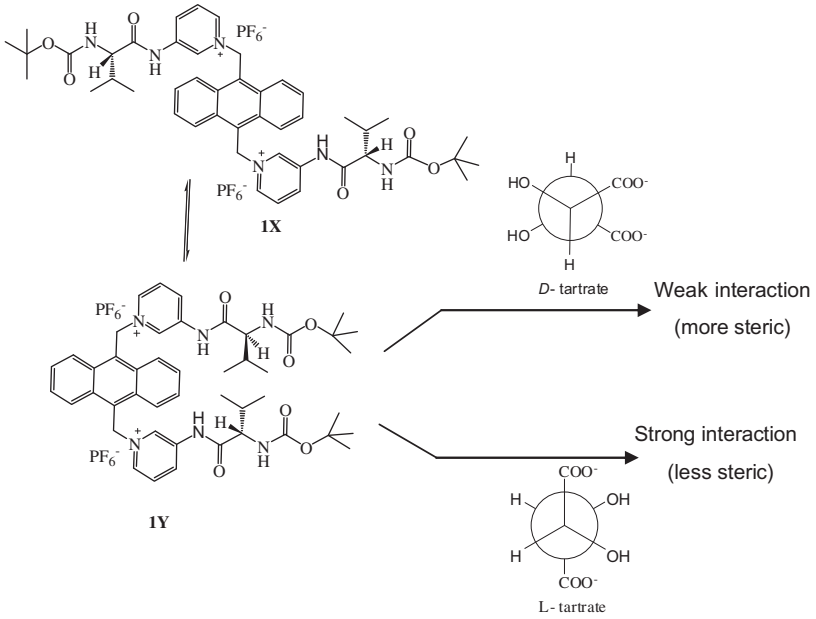

Figure 3. Probable conformations of **1** and their preferential interactions.

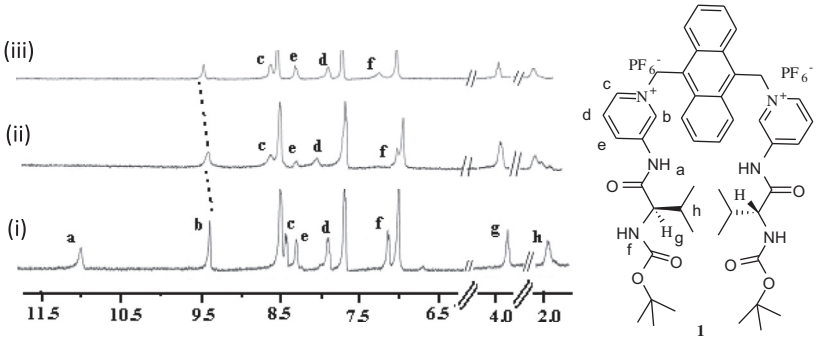

Figure 4. ^{1}H NMR titration of (i) **1** ($c = 2.9 \times 10^{-3}$ M) with (ii) D-tartrate and (iii) L-tartrate.

In the interaction process, the stoichiometry of the complexes of **1** with both D- and L-tartrates was determined to be 1:1 as confirmed by Job plot.[11] Figure 6a, for example, shows the Job plot for **1** with L-tartrate. Non linear fitting of the emission titration data gave the binding constant (K_a)[11] value of $(6.31 \pm 0.05) \times 10^3$ M^{-1} for L-tartrate (Fig. 6b). However, non linear fitting of the emission titration data obtained from the progressive addition of D-tartrate upto 5 equiv amounts introduced K_a value of $(8.18 \pm 0.55) \times 10^2$ M^{-1}, which is less compared to the case with L-tartrate. The emission titration data beyond the addition of 5 equiv amounts of D-tartrate did not fit well in non linear equation to give any reliable binding constant value. The binding constant (K_a) values[12] for the complexes of **1** with *R*- and *S*-mandelate were determined to be $(2.79 \pm 0.39) \times 10^3$ M^{-1} and $(2.07 \pm 0.22) \times 10^3$ M^{-1}, respectively, (Supporting information).

The selective recognition effect of a particular chiral isomer was understood from the change in emission of **1** while it remains with the mirror image isomer in the solution. As can be seen from Figure 7, D-tartrate-induced change in emission of **1** was further perturbed to the considerable extent upon addition of L-tartrate (Fig. 7a), the reverse one was noticed to be insignificant (Fig. 7b).

The UV–vis study of **1** in the presence of tetrabutylammonium salts of D-/L-tartaric and *R*-/*S*-mandelic acids in DMSO showed marginal change in absorbance for anthracene (Supporting information).

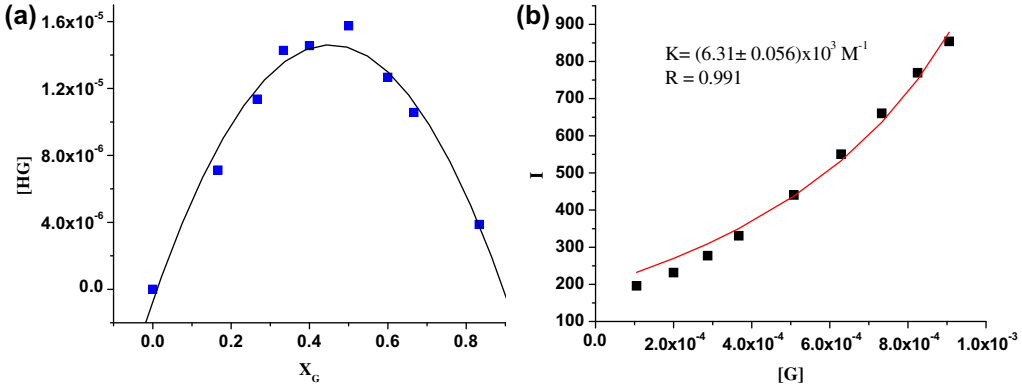

Figure 6. (a) Fluorescence Job plots for **1** with L-tartrate in DMSO ($[H] = [G] = 5.00 \times 10^{-4}$ M); (b) Binding constant curve for **1** with L-tartrate.

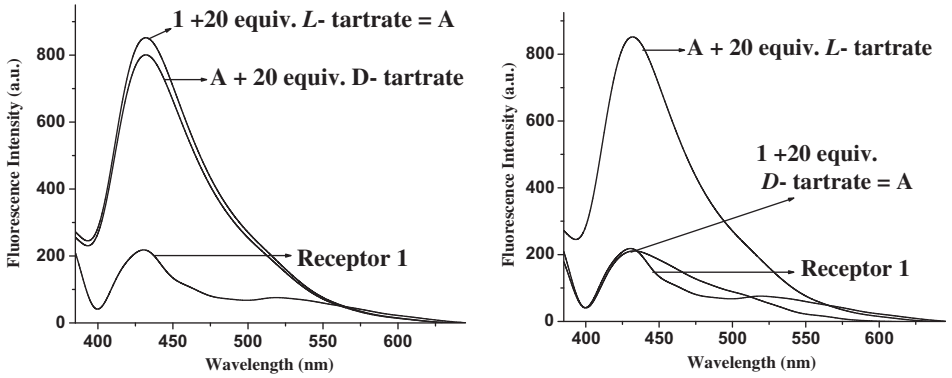

Figure 7. Fluorescent response of receptor **1** ($c = 1.14 \times 10^{-4}$ M) to (a) D-tartrate ($c = 2.2 \times 10^{-3}$ M) in the presence of L-tartrate ($c = 2.2 \times 10^{-3}$ M) and (b) L-tartrate ($c = 2.2 \times 10^{-3}$ M) in the presence of D-tartrate ($c = 2.2 \times 10^{-3}$ M) in DMSO.

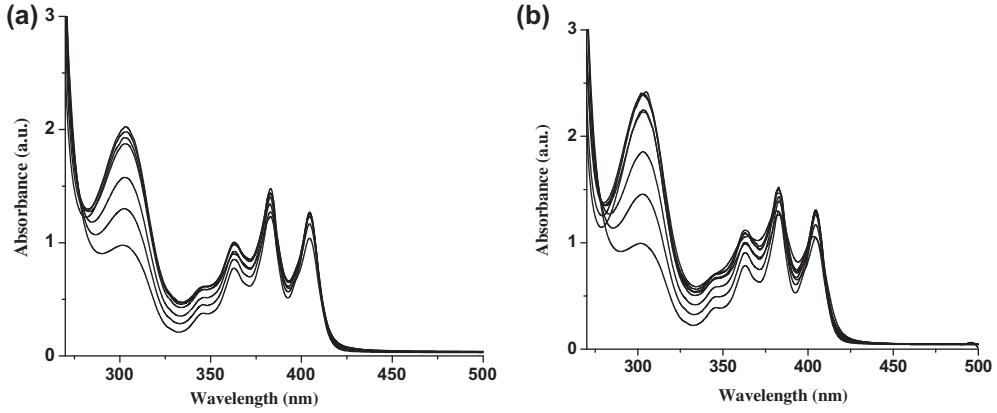

Figure 8. Change in absorbance of **1** ($c = 1.12 \times 10^{-4}$ M) upon gradual addition of (a) L-tartrate, (b) D-tartrate in DMSO.

The change in absorbance in the region ~300 nm (attributed to the pyridinium binding site) was considerable for tartrates (Fig. 8a and b). But no characteristic distinguishable spectral feature was observed in UV.

The stoichiometries of the tartrate complexes with **1** were also 1:1 as determined from Job plot[11] by the UV-method (Supporting information). The binding constant values (K_a) for the isomers of tartrate with **1** were determined to be $(9.56 \pm 2.3) \times 10^3\ M^{-1}$ and $(8.55 \pm 1.9) \times 10^3\ M^{-1}$ for D- and L-tartrates, respectively. This small difference in K_a values in the ground state is in agreement with the DFT results, shown in Figure 5. Similarly, analysis of the absorption data provided the binding constants (K_a) $(1.47 \pm 0.19) \times 10^3\ M^{-1}$ for *R*-mandelate and $(1.08 \pm 0.24) \times 10^3\ M^{-1}$ for *S*-mandelate.

In conclusion, chemosensor **1** is successfully capable of discriminating L-tartrate from D-tartrate fluorimetrically with an '*ef*' value of 29.38. The mandelates being smaller in size than tartrate are unable to bridge the two pyridinium motifs in **1** and thereby induce small change in emission without showing any measurable distinctive feature. The bridging of the two binding arms in **1** by isomeric tartrates induces differential hydrogen bonding perturbation due to which substantial change in emission takes place and L-tartrate is selectively distinguished from its mirror image isomer. However, the use of pyridinium motif in devising such simple receptor for chiral recognition of tartrate is a first time approach after a recent report on lactate recognition[13] by pyridinium-based receptor from our laboratory.

Acknowledgments

We thank the DST New Delhi, India for financial support [project SR/S1/OC-76/2010(G); Date: 23.08.2011]. T.S. thanks the CSIR, New Delhi, India for a fellowship.

Supplementary data

Supplementary data (figures showing the change in fluorescence and UV–vis titrations of receptor **1** with the anions, binding constant curves, Job plots, fluorescence decay spectra, experimental procedure, ^1H, ^{13}C NMR, and mass spectra) associated with this article can be found, in the online version, at http://dx.doi.org/10.1016/j.tetlet.2014.01.016.

References and notes

1. (a) Lin, J.; Hu, Q.-S.; Xu, M.-H.; Pu, L. *J. Am. Chem. Soc.* **2002**, *124*, 2088–2089; (b) Garten, S.; Biedermann, P. U.; Topiol, S.; Agranat, I. *Chirality* **2010**, *22*, 662–674; (c) Ogoshi, H.; Mizutani, T. *Acc. Chem. Res.* **1998**, *31*, 81–89; (d) Schmidtchen, F. P. *Top. Curr. Chem.* **2005**, *255*, 1–30; (e) Pu, L. *Acc. Chem. Res.* **2012**, *45*, 150–163; (f) Pu, L. *Chem. Rev* **2004**, *104*, 1687–1716.
2. (a) Pu, L. *Chem. Rev.* **1998**, *98*, 2405–2494; (b) Gunnlaugsson, T.; Glynn, M.; Tocci, G. M.; Kruger, P. E.; Pfeffer, F. M. *Coord. Chem. Rev.* **2006**, *250*, 3094–3117; (c) Li, Z. B.; Lin, J.; Qin, Y. C.; Pu, L. *Org. Lett.* **2005**, *7*, 3441–3444.
3. Enantioselective recognition of α-hydroxyl carboxylic acids: (a) Chi, L.; Zhao, J.; James, T. D. *J. Org. Chem.* **2008**, *73*, 4684–4687; (b) Xu, M.-H.; Lin, J.; Hu, Q.-S.; Pu, L. *J. Am. Chem. Soc.* **2002**, *124*, 14239; (c) Altava, B.; Burguete, M. I.; Carbo, N.; Escorihuela, J.; Luis, S. V. *Tetrahedron: Asymmetry* **2010**, *21*, 982–989; (d) Lin, J.; Zhang, H.-C.; Pu, L. *Org. Lett.* **2002**, *4*, 3297–3300; (e) Mei, X.; Wolf, C. *J. Am. Chem. Soc.* **2004**, *126*, 14736–14737; (f) Hernandez-Rodriguez, M.; Juaristi, E. *Tetrahedron* **2007**, *63*, 7673–7678; (g) Wu, Y.; Guo, H.; James, T. D.; Zhao, J. *J. Org. Chem.* **2011**, *76*, 5685–5695; (h) Yang, X.; Liu, X.; Shen, K.; Fu, Y.; Zhang, M.; Zhu, C.; Cheng, Y. *Org. Biomol. Chem.* **2011**, *9*, 6011–6021. and references cited therein.
4. (a) Yang, D.; Li, X.; Fan, Y.-F.; Zhang, D.-W. *J. Am. Chem. Soc.* **2005**, *127*, 7996–7997; (b) Duke, R. M.; Gunnlaugsson, T. *Tetrahedron Lett.* **2007**, *48*, 8043–8047; (c) Coppola, G. M.; Schuster, H. F. *α-Hydroxyl Acids in Enantioselective Synthesis*; VCH: Weinheim, Germany, 1997.
5. (a) Han, F.; Chi, L.; Liang, X.; Ji, S.; Liu, S.; Zhou, F.; Wu, Y.; Han, K.; Zhao, J.; James, T. D. *J. Org. Chem.* **2009**, *74*, 1333–1336; (b) Zhao, J.; Fyles, T. M.; James, T. D. *Angew. Chem., Int. Ed.* **1994**, *43*, 3461–3464; (c) Zhao, J.; James, T. D. *Chem. Commun* **2005**, 1889–1891; (d) Ghosh, K.; Adhikari, S. *Tetrahedron Lett.* **2006**, *47*, 3577–3581; (e) Goswami, S. P.; Ghosh, K.; Mukherjee, R. *Tetrahedron* **2001**, *57*, 4987–4993; (f) Hernandez, J. V.; Almaraz, M.; Raposo, C.; Martin, M.; Lithgow, A.; Crego, M.; Caballero, C.; Moran, J. R. *Tetrahedron Lett.* **1998**, *39*, 7401–7404.
6. (a) Bencini, A.; Coluccini, C.; Garau, A.; Giorgi, C.; Lippolis, V.; Messori, L.; Pasini, D.; Puccioni, S. *Chem. Commun.* **2012**, *48*, 10428–10430; (b) Qin, H.; He, Y.; Hu, C.; Chen, Z.; Hu, L. *Tetrahedron Asymmetry* **2007**, *18*, 1769–1774; (c) Jadhav, V. D.; Schmidtchen, F. P. *Org. Lett.* **2006**, *8*, 2329–2332; (d) Lavigne, J. J.; Anslyn, E. V. **1999**, *38*, 3666–3669; (e) Zhao, J.; Davidson, M. G.; Mahon, M. F.; Kohn, G. K.; James, T. D. *J. Am. Chem. Soc.* **2004**, *126*, 16179–16186.
7. Ghosh, K.; Sarkar, T. *Tetrahedron Lett.* **2013**, *54*, 4568–4573.
8. Xu, Z.; Kim, S.; Lee, K.-H.; Yoon, J. *Tetrahedron Lett.* **2007**, *48*, 3797–3800.
9. Ghosh, K.; Masanta, G.; Chattopadhyay, A. P. *Tetrahedron Lett.* **2007**, *48*, 6129–6132.
10. DFT calculation was done by using Gaussian 09 (Revision A.02): Frisch, M. J.; Trucks, G. W.; Schlegel, H. B.; Scuseria, G. E.; Robb, M. A.; Cheeseman, J. R.; Montgomery, J. A.; Vreven, T., Jr.; Kudin, K. N.; Burant, J. C.; Millam, J. M.; Iyengar, S. S.; Tomasi, J.; Barone, V.; Mennucci, B.; Cossi, M.; Scalmani, G.; Rega, N.; Petersson, G. A.; Nakatsuji, H.; Hada, M.; Ehara, M.; Toyota, K.; Fukuda, R.; Hasegawa, J.; Ishida, M.; Nakajima, T.; Honda, Y.; Kitao, O.; Nakai, H.; Klene, M.; Li, X.; Knox, J. E.; Hratchian, H. P.; Cross, J. B.; Adamo, C.; Jaramillo, J.; Gomperts, R.; Stratmann, R. E.; Yazyev, O.; Austin, A. J.; Cammi, R.; Pomelli, C.; Ochterski, J. W.; Ayala, P. Y.; Morokuma, K.; Voth, G. A.; Salvador, P.; Dannenberg, J. J.; Zakrzewski, V. G.; Dapprich, S.; Daniels, A. D.; Strain, M. C.; Farkas, O.; Malick, D.; Rabuck, A. D.; Raghavachari, K.; Foresman, J. B.; Ortiz, J. V.; Cui, Q.; Baboul, A. G.; Clifford, S.; Cioslowski, J.; Stefanov, B. B.; Liu, G.; Liashenko, A.; Piskorz, P.; Komaromi, I.; Martin, R. L.; Fox, D. J.; Keith, T.; Al-Laham, M. A.; Peng, C. Y.; Nanayakkara, A.; Challacombe, M.; Gill, P. M. W.; Johnson, B.; Chen, W.; Wong, M. W.; Gonzalez, C.; Pople, J. A. *DFT Calculation was done by Using Gaussian 09 (Revision A.02)*; Gaussian, Inc.: Wallingford CT, 2004.
11. Job, P. P. *Ann. Chim.* **1928**, *9*, 113–203.
12. Valeur, B.; Pouget, J.; Bourson, J.; Kaschke, M.; Eensting, N. P. *J. Phys. Chem.* **1992**, *96*, 6545–6549.
13. Ghosh, K.; Majumdar, A. *Tetrahedron Lett.* **2013**, *54*, 5686–5689.